

Receding Hamiltonian-Informed Optimal Neural Control and State Estimation for Closed-Loop Dynamical Systems

Josue N. Rivera, Dengfeng Sun

School of Aeronautics and Astronautics

Purdue University

West Lafayette, IN 47907, USA

{RIVER264, DSUN}@PURDUE.EDU

Abstract

This paper formalizes Hamiltonian-Informed Optimal Neural (Hion) controllers, a novel class of neural network-based controllers for dynamical systems and explicit non-linear model predictive control. Hion controllers estimate future states and compute optimal control inputs using Pontryagin’s Maximum Principle. The proposed framework allows for customization of transient behavior, addressing limitations of existing methods. The Tailored Multi-Faceted Approach for Neural ODE and Optimal Control (T-mano) architecture facilitates training and ensures accurate state estimation. Optimal control strategies are demonstrated for both linear and non-linear dynamical systems.

Keywords: model-predictive control, neural control, control theory, physics-informed neural network

1 Introduction

Optimal control problems often involve designing controllers for systems with complex, chaotic, and/or non-linear dynamics. These problems are crucial in sectors such as unmanned aerial vehicles (UAVs) flight controllers, robotics, and nuclear power plants (Salzmann et al., 2023; Katayama et al., 2023; Naimi et al., 2022). Various methods have been developed to address these problems. Solutions include dynamic programming, bang-bang controllers, proportional-integral-derivative (PID) controllers, linear-quadratic regulators (LQR), reinforcement learning (RL), and many variants of model predictive control (MPC). However, these methods often encounter challenges in delivering solutions that are both optimally effective and practical. Some methods react to deviations without considering the optimality of the control, while others can be expensive to operate in practice (Schwenzer et al., 2021; Bemporad et al., 2002). Neural network approaches also grapple with their own unique challenges to generate solutions that consider accurate system dynamics. The quality of the control is often contingent on the quality of the training data (Zheng et al., 2023). Among the developed methods, MPC is intriguing as it considers the effects of current control actions on future states. Nonetheless, many methods fail to address optimality conditions or computational efficiency when real-time optimization of the control is required (Bemporad et al., 2002).

To address these challenges, this chapter introduces a new class of neural network-based controllers for dynamical systems: Hamiltonian-Informed Optimal Neural (Hion) controllers, along with a novel architecture, the Tailored Multi-Faceted Approach for Neural ODE and Optimal Control (T-mano). Hion controllers are a type of explicit MPC neural network-based models that map an observed and desired state to a continuous con-

trol strategy and expected future states. The objective is to optimize the parameters of the controller to provide state estimation and control that not only adheres to a system dynamics but also follows a given transient response profile. The model is intended to operate in a closed-loop system, where it can cope with delays in receiving state information by predicting the system’s expected future behavior. Hion controllers offer a new alternative to RL methods and other MPC-based approaches for controlling dynamical systems such as UAVs and other robots.

1.1 Background

Model-predictive control (MPC) defines a set of algorithms that utilize future state estimation to generate control strategies for a system (Schwenzer et al., 2021). They often involve iteratively solving control optimization problems for a receding horizon in a closed-loop environment. Classical MPCs repeatedly linearize the plant’s dynamics at each iteration. These are used for state prediction and to solve for a zero-order hold control strategies via dynamic programming. The linearization-based approach enables computationally effective state estimation, albeit at the expense of some dynamic accuracy. Non-linear MPCs (NMPCs) are a later attempt to incorporate the dynamics non-linearity by using surrogate models to reduce the computational burden of state predictions. Explicit MPCs form an overlapping category that solve the control optimization in advance and reuse the previously obtained solution when tested (Schwenzer et al., 2021; Bemporad et al., 2002). Our proposed controller falls under the category of an explicit NMPC.

Artificial neural networks with MPC (ANN-MPC) are a subset of MPC models that most often involve utilizing neural networks as the prediction models in a MPC-based control loop (Wang et al., 2021; Pang et al., 2023; Hewing et al., 2020; Cavagnari et al., 1999). Commonly, they consist of training a neural network model to predict that expected future state of system after a given amount of time, relying on trajectories data collected in simulation or test environments. The advantage of these models is that they can reduce significantly the cost of classical computationally expensive prediction model with the approximation provided by the neural network. Hence, less time is needed before the next state of the system can be sampled and an action could be taken. Recurrent neural networks are used in a subset of these algorithms (Jordanou et al., 2021; Ren et al., 2022). They involve feeding previously sampled state to the model during inference and passing its knowledge to future generation to improve its predictive capability. Although a significant number of strategies involve replacing the predictive component, a subset of these works attempt to replace the MPC controller entirely by training them to be surrogate using collected trajectories and the corresponding control observed by a larger computationally-expensive MPC model (Rivera et al., 2024; Hertneck et al., 2018; Åkesson and Toivonen, 2006). However, the optimality, dynamics accuracy, and out-of-distribution performance can be impacted when using neural networks as surrogate models.

Physics-informed neural network with MPC (PINN-MPC) seeks to improve even further the capability of the predictive models in the MPC loop. At their core, PINN-MPCs integrate information about the dynamics that result in improvement to the accuracy and precision of the future state estimation and the information passed to the control optimization (Antonelo et al., 2024; Faria et al., 2024; Arnold and King, 2021; Zheng et al., 2023).

Physics-Informed Neural Nets for Control (PINC), introduced in (Antonelo et al., 2024), was one of the first method proposed to use PINNs as the prediction model in a MPC strategy. It consist of training a PINN to predict an continuous estimation of future states for a fixed horizon given a constant control signal. With this method, more reliable prediction exists that can guide a control optimization. Additionally, due to the continuous state prediction, distinct control optimization strategies that rely on distinct sampling rate can be implemented or tested with a single PINN model. Limitations exist with these approaches. Although, a continuous set of future states of the system are estimated, PINN-MPCs often rely on a single predicted state to guide the control, due to the model reliance on zero-order hold control optimization.

Few works exist that consider neural networks as physics-informed controller in dynamical systems. Fewer works exist that allow for the adjustment of the environment transient characteristic. Ours and newer approaches reinvents the idea of a controller when a neural network model is involved. (Schiassi et al., 2022) illustrate the feasibility of training neural controllers using Bellman optimality principle, and how they can be extended using X-TFC for different initial and final conditions. (Schiassi et al., 2021). (D’ambrosio et al., 2021; Barry-Straume et al., 2022; Chi, 2024) are recent attempts to establish neural network models that encourages PMP optimality. The works demonstrated that PMP can be used to train a neural network model to predict an optimal trajectory with desired transient properties. However, several limitations exist. One such limitation is that each model was only demonstrated to solve TVBNP for a single predefined initial and final state. This makes them impractical for closed-loop systems control where they will vary. Any new boundary condition would require fine-tuning the model (e.g., using X-TFC). Building on top of these projects, our model provides a closed-loop MPC neural network-based controller and state estimator that generalizes for variable inputs. It also theoretically defines a set of dynamical systems for which the model may be utilized. Hion removes the classical control optimization step conducted by classical MPC models, ANN-MPC, and PINN-MPC, and use a single neural network as both the prediction and control model.

Fig. 1 illustrates a comparison between the conceptual behavior of different model predictive controllers.

1.2 Contributions

Our research formalizes a novel class of neural network controllers, termed Hion controllers, designed to optimize control strategies within closed-loop dynamical systems. These controllers function as model predictive controllers, enabling predictive decision-making. Our contributions include:

1. Establishing a theoretical framework for Hion controllers.
2. Proposing a novel neural network architecture specifically tailored for state estimation and control of dynamical systems.
3. Developing algorithms for training Hion controllers that are aligned with Pontryagin’s Maximum/Minimum Principle and encourage optimal control.

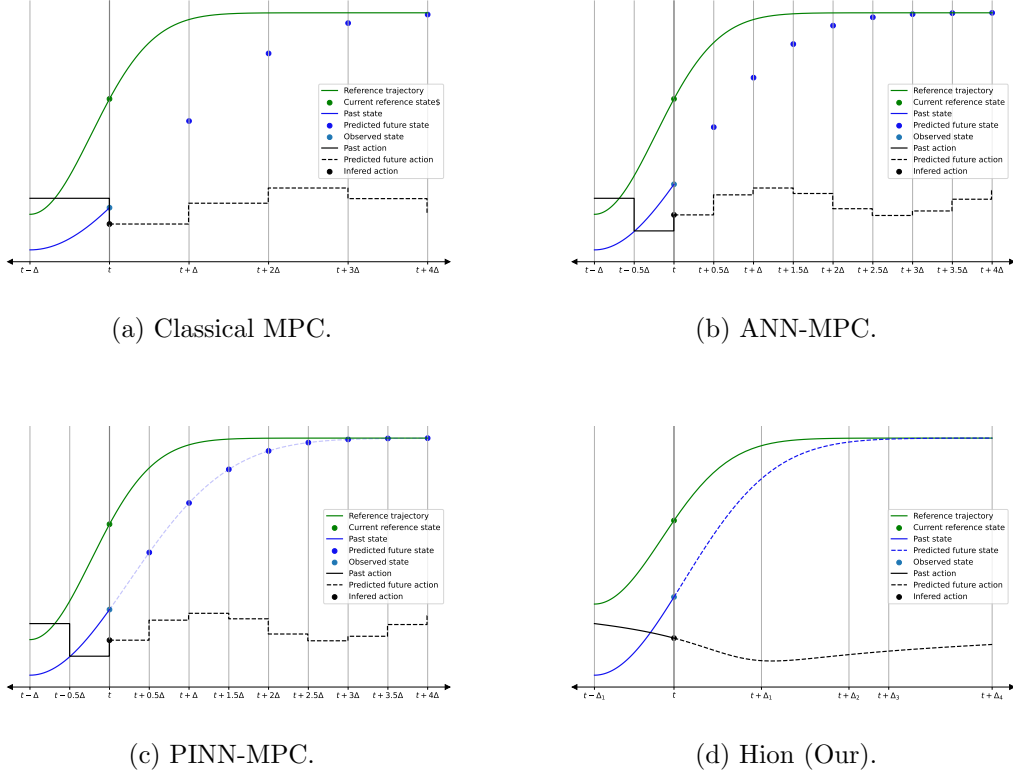


Figure 1: Conceptual behaviors of closed-loop model predictive controllers.

1.3 Outline

Following the introduction, the first section formally defines the problem of interest we aim to address. We then present our proposed methodology and the underlying theoretical principles that support it. The experimental results section demonstrates the effectiveness and capabilities of our architecture through its application to various dynamical systems. Finally, we conclude by highlighting the advantages and limitations of the method along with potential future directions of our work.

2 Problem Statement

Consider a general dynamical system (or environment) with ordinary differential equations (ODEs) and a corresponding state-space representation describing it,

$$\begin{aligned} \mathcal{F}(t, \bar{x}(t), u(t)) &= 0 \\ \dot{x}(t) &= f(t, x(t), u(t)) \end{aligned} \quad (1)$$

where t represents time, $x(t)$ the state vector of the environment, $\bar{x}(t)$ the state vector in addition to some higher-order derivatives w.r.t. time needed to describe the ODEs, $u(t)$ the control action vector, \mathcal{F} the ODEs describing the dynamics, and f the dynamics function. Note $\dot{x}(t) = \frac{d}{dt}x(t)$.

Definition 1 (Hion Controller) Let *Hamiltonian-Informed Optimal Neural (Hion) controllers* be a class of neural networks models $h : \mathbb{R} \times \mathbb{R}^n \times \mathbb{R}^n \rightarrow \mathbb{R}^k \times \mathbb{R}^m \times \mathbb{R}^n$ that maps the elapsed time \hat{t} since a state was last observed, the last observed state $x_o := x(t - \hat{t})$, and a reference state $x_r(t)$ to an inferred state $x_h(t)$, control $u_h(t)$, and co-state (i.e., Lagrange multiplier) $\lambda_h(t)$. As a neural network, h contains a set of learnable parameters μ .

Given a transient cost to influence the behavior of the system and defined by the Lagrangian function L

$$J = \int_0^{\infty} L(t, x(t), x_r(t), u(t)) dt \quad (2)$$

, the **problem of interest** is to optimize a Hion controller's parameters μ to provide an optimal control strategy u_h that reduces the least-square-error (LSE) between expected future states of the system x_h and the current reference state x_r while adhering to the dynamics of the system (1) and, secondarily, minimizing the transient cost (2). The LSE with respect to the reference condition may be omitted if a reference is not required by the problem at hand.

3 Methodology

Our proposed optimization for a Hion controller consists of three major components: a distribution for observed and reference states, the Hion controller, and a set of criterion based on Pontryagin's Minimum/Maximum Principle (PMP). The state distribution defines random variable vectors from which inputs to the model can be sampled that aid in the converge of the controller. The controller defines the structure of the model and provides inferred states, controls, and their corresponding co-states. Lastly, the criterion evaluates the controller and the parameters μ are updated, accordingly. An overview of the methodology is presented in Figure 2.

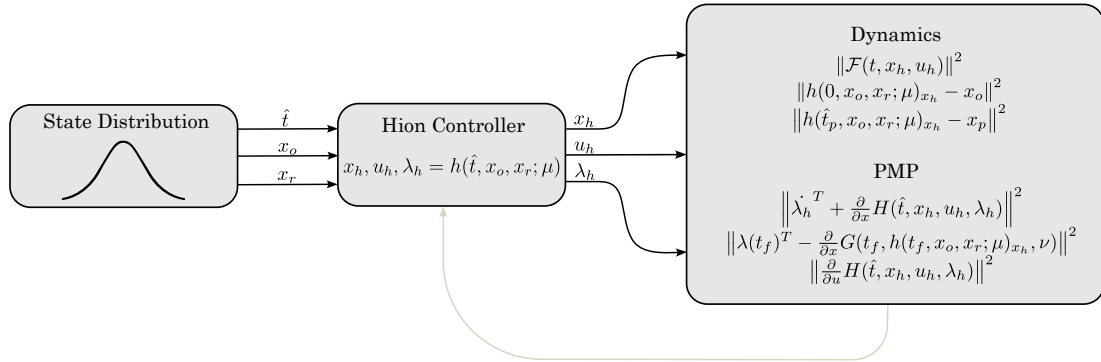


Figure 2: Hion Controller Training Flowchart

3.1 State Distribution

Following the convection set forth by PINNs (Hao et al., 2022), the inputs to the Hion model are sampled from random variables. The first input, the elapsed time \hat{t} , is sampled from an uniform distribution,

$$\hat{T} \sim \mathcal{U}(0, t_f) \quad (3)$$

where t_f is a terminal time. In a two point boundary value problem (TPBVP), t_f indicates the final time of the problem. In a closed-loop system, it represents the size of the window for the system to be driven to a reference state. For the other inputs to the model, we must first introduce some definitions and theorems.

Definition 2 (Dynamics invariant to a state transformation) *Let f be a dynamics function and T be a transformation function. The dynamics f is said to be invariant to a transformation T on the state x if and only if for all x , for all other distinct states x' , and for all possible control actions u , the following equality holds:*

$$f(x, x', u) = f(T(x), x', u)$$

This means that the dynamics do not change when the current state x is transformed by T .

From Definition 2, we can introduce the following theorems.

Theorem 3 *The following statements are equivalent:*

- (A) *The dynamics are invariant under all transformation T applied to the state x .*
- (B) *The dynamics function f explicitly does not depend on the state x .*
- (C) *Without loss of generality, a state x in a dynamic function f can always be assumed to be fixed at a particular value.*

Proof (A) \Rightarrow (B): If the dynamics are invariant under all transformations T applied to the state x , then by definition, for any transformation T on the state x , the dynamics function $f(x, x', u)$ satisfies $f(x, x', u) = f(T(x), x', u)$ for all x , for all other states x' , and for all possible control actions u . This implies that the dynamics equation f explicitly does not depend on the state x , because the dynamics remain the same even when x is transformed by any T . Hence, $f(x, x', u) = F(x', u)$ and $f(T(x), x', u) = F(x', u)$ where $F(x', u)$ does not depend on x .

(B) \Rightarrow (C): If the dynamics equation f describing the system does not contain the state x , it means that the dynamics are the same for any state x . Therefore, without loss of generality, we can always choose our state x so that it is always fixed a particular value.

(C) \Rightarrow (A): If, without loss of generality, the state x can always be assumed to be fixed at a particular value in a dynamics function, then when we can apply any transformation T on the state x , and the assumption would still hold. Thus, the dynamics remain the same $f(x, x', u) = f(T(x), x', u)$. Hence, by definition, the dynamics are invariant to a transformed state x .

Therefore, we have shown that the statements (A), (B), and (C) are equivalent. This completes the proof. ■

Theorem 4 Let $g(x_o, u)$ be the solution to $x(t)$ from the last observed state x_o of the system and given the control actions u during the elapse time. If the dynamics are invariant to all transformation T on the state \bar{x} , then

$$g \begin{matrix} \bar{x}_o \\ x'_o \end{matrix}, u = g \begin{matrix} \bar{x}_o - \Delta_x \\ x'_o \end{matrix}, u + \begin{matrix} \Delta_x \\ 0 \end{matrix}$$

where Δ_x is some value, and x' all other distinct states.

Proof By Taylor expansion, the solution $g(x_o, u)$ can be expressed as,

$$\begin{aligned} g(x_o, u) &= g \begin{matrix} \bar{x}_o \\ x'_o \end{matrix}, u = \begin{matrix} \bar{x}_o \\ x'_o \end{matrix} + f(\bar{x}_o, x'_o, u) \hat{t} + \frac{\dot{f}(\bar{x}_o, x'_o, u)}{2!} \hat{t}^2 + \sum_{n=3}^{\infty} \frac{f^{(n-1)}(\bar{x}_o, x'_o, u)}{n!} \hat{t}^n \\ &= \begin{matrix} \bar{x}_o - \Delta_x \\ x'_o \end{matrix} + f(\bar{x}_o, x'_o, u) \hat{t} + \frac{\dot{f}(\bar{x}_o, x'_o, u)}{2!} \hat{t}^2 + \sum_{n=3}^{\infty} \frac{f^{(n-1)}(\bar{x}_o, x'_o, u)}{n!} \hat{t}^n + \begin{matrix} \Delta_x \\ 0 \end{matrix} \end{aligned}$$

Given the dynamics are invariant to all transformation T on the state \bar{x} , by Definition 2 and Theorem 3, $f(\bar{x}_o, x'_o, u) = f(\bar{x}_o - \Delta_x, x'_o, u)$ and $f^{(i)}(\bar{x}_o, x'_o, u) = f^{(i)}(\bar{x}_o - \Delta_x, x'_o, u)$ for any i^{th} derivative w.r.t. time and any arbitrary value Δ_x . Hence,

$$\begin{aligned} g(x_o, u) &= \begin{matrix} \Delta_x^o \\ x'_o \end{matrix} + f(\bar{x}_o, x'_o, u) \hat{t} + \frac{\dot{f}(\bar{x}_o, x'_o, u)}{2!} \hat{t}^2 + \sum_{n=3}^{\infty} \frac{f^{(n-1)}(\bar{x}_o, x'_o, u)}{n!} \hat{t}^n + \begin{matrix} \Delta_x \\ 0 \end{matrix} \\ &= \begin{matrix} \Delta_x^o \\ x'_o \end{matrix} + f(\Delta_x^o, x'_o, u) \hat{t} + \frac{\dot{f}(\Delta_x^o, x'_o, u)}{2!} \hat{t}^2 + \sum_{n=3}^{\infty} \frac{f^{(n-1)}(\Delta_x^o, x'_o, u)}{n!} \hat{t}^n + \begin{matrix} \Delta_x \\ 0 \end{matrix} \\ &= g \begin{matrix} \Delta_x^o \\ x'_o \end{matrix}, u + \begin{matrix} \Delta_x \\ 0 \end{matrix} \\ &= g \begin{matrix} \bar{x}_o - \Delta_x \\ x'_o \end{matrix}, u + \begin{matrix} \Delta_x \\ 0 \end{matrix} \end{aligned}$$

where $\Delta_x^o := \bar{x}_o - \Delta_x$.

Therefore, we have shown that,

$$g \begin{matrix} \bar{x}_o \\ x'_o \end{matrix}, u = g \begin{matrix} \bar{x}_o - \Delta_x \\ x'_o \end{matrix}, u + \begin{matrix} \Delta_x \\ 0 \end{matrix}$$

for any arbitrary value Δ_x . This completes the proof. ■

With the theorems at hand, when training a Hion controller, we assume that the observed state's x_o input must adhere to Assumption 4.1.

Assumption 4.1 (Observed State Condition) *If a Hion controller converges to a set of parameter μ via parameters optimization while adhering to the dynamics f , then each observed state of the system must have either: (1) been sampled from a random variable with a proper distribution, or (2) the dynamics of the system are invariant to all transformation T on the state.*

The intuition behind Assumption 4.1 is that if an observed state corresponding random variable does not have a proper distribution, then training the model via sampling from the distribution may not converge. However, if the dynamics are invariant to all transformation on a given state, then during training, the observed state can be assigned some fixed particular value by Theorems 3 and 4 assuming the dynamics hold for the inferred states x_h and controls u_h . For inference, the invariant state can be fixed to the particular value, then the solution can be readjusted via Theorem 4. An example of states in a system that would satisfy the invariant property would be position in the unconstrained quadcopter dynamics (Abougarair et al., 2024). States in an unconstrained resource allocation optimal control problem (i.e., queen-worker insect problem) do not or have a proper distribution (Winkel, 2013; Oster and Wilson, 1978).

The reference state’s x_r sampled for training are chosen from a random variable \mathbf{X}_r that depends on the observed state training input’s random variable \mathbf{X}_o . Unless otherwise considered, a reference state is always assumed to be feasible or nearly feasible to allow for tracking in a short time span. As such, if the state is continuous and unconstrained, the reference state input random variable can be assumed, to be

$$\mathbf{X}_r = x_o^r + \mathbf{E}, \quad \mathbf{E} \sim \mathcal{N}(0, \sigma^2)$$

where x_o^r is the subset of the observed states relevant to the reference, and σ^2 defines the variance of the reference states with respect to the observed states.

3.2 Controller Architecture

As presented in the problem statement, a Hion controller $h(\cdot)$ is described by,

$$x_h, u_h, \lambda_h = h(\hat{t}, x_o, x_r; \mu) \tag{4}$$

where elapsed time \hat{t} , last observed state x_o , and reference state x_r describe the inputs to the model, sampled from a distribution. On the other hand, the expected state x_h , corresponding control u_h , and co-state (i.e., Lagrange multiplier) λ_h describe the generative output. μ is the set of parameters dictating the behavior of the model.

As it is desired that the neural network adhere to the dynamics and akin to PINN models, primitive states (i.e., zero-order derivative state w.r.t. time) $x_{[0]}^h$ and controls $u_{[0]}^h$ are inferred. Any higher-order derivative state is obtained by,

$$x_{[i+1]}^h = \dot{x}_{[i]}^h = x_{[0]}^h \stackrel{(i)}{=} \frac{\partial}{\partial \hat{t}} x_{[i]}^h \quad u_{[i+1]}^h = \dot{u}_{[i]}^h = u_{[0]}^h \stackrel{(i)}{=} \frac{\partial}{\partial \hat{t}} u_{[i]}^h \tag{5}$$

The output of the model, x_h and u_h , denote the vector of the states $x_{[i]}^h$ and controls $u_{[i]}^h$ relevant to the system, respectively. These may, however, not follow accurate dynamics or be optimal when modeled by a conventional neural network model.

3.2.1 TAYLORED MULTI-FACETED APPROACH FOR NEURAL ODE AND OPTIMAL CONTROL

The **problem of interest** present unique opportunity to build a neural network architecture tailored for the task. Taylored Multi-Faceted Approach for Neural ODE and Optimal

Control (T-mano) is a novel architecture for optimal control and state estimation of dynamical systems based on Taylor expansion. It ensures that initial conditions and accuracy of some of the systems dynamics are maintained in inference regardless of the parameters optimization. The architecture is presented in Fig. 3 and consists of four main stages.

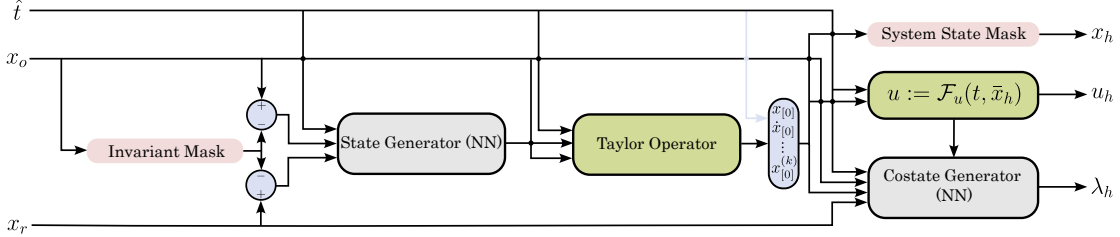


Figure 3: T-Mano Architecture for Control. It consists of four main stages that ensure that initial conditions and partial dynamics accuracy are maintained.

Initially, the invariant mask filters observed states that are considered invariant to all transformation under Definition 2 and fixes them to zero before the state generator. The results does not affect the inference of the model as a solution to the system was proven to generalize to other invariant states in Theorem 4 when fixed to a value. However, fixing these invariant states to a value (e.g., zero in this case) was empirically found to improve convergence and generalization to out-of-distribution invariant states.

In the first main stage, the state generator (as a neural network) provides a higher-order terms state function $\hat{x}_h(\hat{t})$ to the Taylor operator before any future states are inferred. It is modeled by a multi-layer perceptron (MLP),

$$\begin{aligned} \hat{x}_h &= h_x(\hat{t}, \bar{x}_o, \bar{x}_r; \mu_x) = (h_k \circ \sigma \circ \dots \circ h_2 \circ \sigma \circ h_1)(\hat{t}, \bar{x}_o, \bar{x}_r) \\ h_j(z) &= W_j z + b_j \end{aligned} \quad (6)$$

where $\mu_x = \{W_1, b_1, \dots, W_k, b_k\}$ is the set of all the learnable parameters of the model, and $\sigma(\cdot)$ is the non-linear activation function. For the experiments explored, $\sigma(\cdot) = \text{SiLU}(\cdot)$.

The Taylor operator $\mathcal{T}(\cdot)$ is a mapping of the observed state x_o and a higher-order terms state function $\hat{x}(\hat{t})$ to a state estimation that ensure that the initial condition of the system x_o is respected. It is defined as:

$$\mathcal{T}(\hat{t}, x_o, \hat{x}(\hat{t})) = \sum_{n=0}^{k-1} \frac{x_{[n]}^o}{n!} \hat{t}^n + \hat{x}(\hat{t}) \hat{t}^k \quad (7)$$

where $x_{[i]}^o$ represents the i^{th} -order derivatives w.r.t. time of the primitive state $x_{[0]}^o$ in the observed states x_o , $k - 1$ is the highest known order, and $\hat{x}(\hat{t})$ is a higher-order terms state function. In the architecture, the higher-order terms state function is provided by the state generator $\hat{x}_h(\hat{t})$ and the operator is applied to each primitive state.

The theoretical basis for the Taylor operator comes from Taylor expansion that suggests that a solution $x_{[0]}(t)$ to the system can be expressed as:

$$x_{[0]}(t) = x_{[0]}^o + x_{[1]}^o \hat{t} + \frac{x_{[2]}^o}{2!} \hat{t}^2 + \sum_{n=3}^{\infty} \frac{x_{[n]}^o}{n!} \hat{t}^n \quad (8)$$

However, given that observed state only contains $k-1$ known orders of state differentiability, the rest of the higher-order term states must be found. Fortunately, also by Taylor expansion, they can be decomposed to a single unknown function \hat{x} :

$$\begin{aligned}
 x_{[0]}(t) &= x_{[0]}^o + x_{[1]}^o \hat{t} + \frac{x_{[2]}^o}{2!} \hat{t}^2 + \sum_{n=3}^{\infty} \frac{x_{[n]}^o}{n!} \hat{t}^n = \sum_{n=0}^{\infty} \frac{x_{[n]}^o}{n!} \hat{t}^n \\
 &= \sum_{n=0}^{k-1} \frac{x_{[n]}^o}{n!} \hat{t}^n + \sum_{n=k}^{\infty} \frac{x_{[n]}^o}{n!} \hat{t}^n \\
 &= \sum_{n=0}^{k-1} \frac{x_{[n]}^o}{n!} \hat{t}^n + \sum_{n=0}^{\infty} \frac{x_{[n+k]}^o}{(n+k)!} \hat{t}^n \hat{t}^k \\
 &= \sum_{n=0}^{k-1} \frac{x_{[n]}^o}{n!} \hat{t}^n + \sum_{n=0}^{\infty} \frac{n! x_{[n+k]}^o}{n!(n+k)!} \hat{t}^n \hat{t}^k \\
 &= \sum_{n=0}^{k-1} \frac{x_{[n]}^o}{n!} \hat{t}^n + \sum_{n=0}^{\infty} \frac{\tilde{x}_{[n]}^o}{n!} \hat{t}^n \hat{t}^k \\
 &= \sum_{n=0}^{k-1} \frac{x_{[n]}^o}{n!} \hat{t}^n + \hat{x}(\hat{t}) \hat{t}^k
 \end{aligned} \tag{9}$$

where $\tilde{x}_{[n]}^o := \frac{n! x_{[n+k]}^o}{(n+k)!}$ and $\hat{x}(\hat{t})$ is the unknown higher-order terms state function.

After the Taylor operator, a vector of state prediction \bar{x}_h can be obtained via differentiation of the inferred primitive states $x_{[0]}^h$ w.r.t. the elapse time \hat{t} as described in Eq. (5). A subset of these states x_h is outputted as the system state prediction.

The control definition serves as the third main stage. In this stage, the control u_h is defined using the ODEs and the vector of high-order state estimations \bar{x}_h . It is described in a way that no residual exists between the estimation of the states and the dynamics of the system for ODEs that contain a control point. The control can be interpreted as a relation of the system states.

$$u_h := \mathcal{F}_u(t, \bar{x}_h) \tag{10}$$

Now that a state estimation is inferred and the control associated with it is defined, the final stage is to generate a set of co-states to guide the optimality. The co-state generator is a neural network, that computes the Lagrangian multiplier needed to satisfy PMP. In the experiments presented, it is also modeled by a MLP,

$$\begin{aligned}
 \lambda_h &= h_{\lambda}(\hat{t}, x_o, x_r, \bar{x}_h, u_h; \mu_{\lambda}) = (h_k \circ \sigma \circ \dots \circ h_2 \circ \sigma \circ h_1)(\hat{t}, x_o, x_r, \bar{x}_h, u_h) \\
 h_j(z) &= W_j z + b_j
 \end{aligned} \tag{11}$$

where μ_{λ} is the set of learnable parameters for the co-states generator and $\sigma(\cdot) = \text{SiLU}(\cdot)$.

3.3 Pontryagin’s Maximum/Minimum Principle and Learning Algorithm

Pontryagin’s Maximum/Minimum Principle (PMP) was relied upon to guide the parameters optimization of our neural controller for its computational efficiency. Devised by Lev Pontryagin in the Soviet Union, PMP presents a set of necessary conditions for optimal control of deterministic dynamics (Ma and Zou, 2021; Hwang, 2022; Todorov, 2012, 2006). It can be understood through the method of Lagrange multipliers where a function, known as the Hamiltonian H , is defined that must be maximized/minimized. The function ensured that the system dynamics are respected when considering the Lagrangian L optimization. The optimal control of the system given the Lagrangian is determined by finding the control u that is at an extreme of the Hamiltonian H . Given PMP, necessary conditions for optimality of a controller that drives a system towards a reference state $x_r(t)$ in a TPVBP are:

$$\begin{aligned}\dot{\lambda}(t)^T &= -\frac{\partial}{\partial x}H(t, x(t), u(t), \lambda(t)) \\ \lambda(t_f)^T &= \frac{\partial}{\partial x}G(t_f, x(t_f), \nu) \\ \frac{\partial}{\partial u}H(t, x(t), u(t), \lambda(t)) &= 0\end{aligned}\tag{12}$$

where ν a free variable, and,

$$H(t, x(t), u(t), \lambda(t)) := L(t, x(t), x_r(t), u(t)) + \lambda(t)^T f(t, x(t), u(t))\tag{13}$$

$$G(t_f, x(t_f), \nu) := \nu^T (x(t_f) - x_r(t))\tag{14}$$

In addition to these conditions for optimality, we must also ensure that dynamics of the system are maintained in estimation. Hence, we must also include the environment’s ODEs and boundary as necessary conditions for dynamics accuracy:

$$\begin{aligned}x(0) &= x_o \\ x(t_f) &= x_r(t) \\ \mathcal{F}(t, x(t), u(t)) &= 0\end{aligned}\tag{15}$$

Now that all the conditions for accurate and optimal trajectories are known. They provide us a set of loss functions by mean-square error (MSE) to guide our learning algorithms:

$$\frac{1}{n_x} \|x_h(0) - x_o\|^2\tag{16a}$$

$$\frac{1}{n_{x_r}} \|x_h^r(t_f) - x_r\|^2\tag{16b}$$

$$\frac{1}{n_{\mathcal{F}}} \mathcal{F}(\hat{t}, x_h, u_h)^2\tag{16c}$$

$$\frac{1}{n_x} \lambda_h^T + \frac{\partial}{\partial x}H(\hat{t}, x_h, u_h, \lambda_h)^2\tag{16d}$$

$$\frac{1}{n_{x_r}} \lambda_h^r(t_f)^T^2\tag{16e}$$

$$\frac{1}{n_u} \frac{\partial}{\partial u}H(\hat{t}, x_h, u_h, \lambda_h)^2\tag{16f}$$

where x_h^r and $\lambda_h^r(t_f)$ refers to the associated states and not associated co-states with a reference state, respectively, and n_g defines the dimensionality of some vector g .

However, not all of these losses are needed to train a Hion controller. In the aforementioned T-mano architecture, the Taylor operator ensures that the initial boundary condition for the states is maintained in inference, allowing (16a) not to be required during training. If the problem at hand does not rely on a reference state, then (16a) is also not needed. Additionally, the control definition ensures that any ODE that contains a single control point is satisfied, thus this subset of ODEs do not need to be included in (16c). Lastly, the co-state generator may also be amended to use the Taylor operator, fixing the co-state terminal condition. This would remove the need for (16e).

Following the conversion set forth by PINN models and applying a gradient decent based optimization, Algorithm 1 is used to train and fine-tune our Hion controllers through the differential equations (16). The algorithm initially consists of sampling a number of observed states with individuality dependent references. They represent the start and end of random trajectories for which solutions need to be found at a given epoch. Three time interval are then considered for evaluating the model. First, the controller is evaluated when the elapse time $\hat{t} = 0$. The evaluation is used to measure loss (16a) at which the inferred state $x_h(0)$ must equal the observed state x_o . The second time interval is the terminal time $\hat{t} = t_f$ at which losses (16b) and (16e) are measured. It represents the time at which the reference state must be reached and the boundary condition for the co-states satisfied. Lastly, we consider transient time intervals \hat{t} sampled from an uniform distribution between the boundaries. At these intervals, the transient losses (16c), (16d), and (16f) are measured to ensure that the dynamics and optimality conditions are learned. Note that (16c), (16d), and (16f) may optionally be applied at $\hat{t} = 0$ or $\hat{t} = t_f$ as well. The evaluations of these losses are then used to train the controller via backpropagation and with a chosen optimizer.

Algorithm 1 Training and fine-tuning algorithm for Hion controllers

Require: $n_E, \mu, h(\cdot; \mu), \mathcal{F}(\cdot), f(\cdot), L(\cdot), t_f, \mathbf{X}_o, \mathbf{X}_r$
for n_E epochs **do**
 Sample x_o and x_r from \mathbf{X}_o and \mathbf{X}_r , respectively
 Sample auxiliary elapsed time \hat{t} from $\mathcal{U}(0, t_f)$
 Compute $x_h(0), u_h(0), \lambda_h(0) = h(0, x_o, x_r; \mu)$
 Compute $x_h(t_f), u_h(t_f), \lambda_h(t_f) = h(t_f, x_o, x_r; \mu)$
 Compute $x_h, u_h, \lambda_h = h(\hat{t}, x_o, x_r; \mu)$
 Evaluate and sum the MSE losses relevant to the problem in equation (16) into f_h
 Compute the gradient of f_h w.r.t. μ . i.e., $\frac{\partial f_h}{\partial \mu}$
 Update μ using $\frac{\partial f_h}{\partial \mu}$ and an optimizer ▷ Adam was used for results shown
end for

4 Experiments and Results

To evaluate the capabilities of the proposed architecture T-mano, we will use it to find solutions to the **problem of interest** for a set of dynamical systems (i.e, environments).

4.1 Dynamical Systems

Two systems are considered – one linear and one non-linear. The linear system is a basic unstable second-order linear system that serves as an initial benchmark. The non-linear system is a Van der Pol oscillator. It models an oscillating system with non-linear damping.

SECOND-ORDER LINEAR SYSTEM

Second-order linear system models a range of different phenomena in nature. One such phenomenon is the classical spring-mass problem that explores the movement of a mass attached to a spring as a control force is applied to it over time. For our experiments, we have chosen an unstable system of a car without a spring. It is described by the following ODE,

$$\mathcal{F}(t, \bar{x}(t), u(t)) = \ddot{x}_{[0]} - u = 0 \tag{17}$$

and its corresponding dynamics function,

$$\dot{x} = f(x, u) = \begin{matrix} x_{[1]} \\ u \end{matrix} \tag{18}$$

where $x_{[0]}$ is the primitive state of the second-order linear system (i.e., displacement of the mass) and u is an applied force over time.

For the observed state distribution used to train the hion controller, we have chosen the following random state vector:

$$\mathbf{X}_o = \begin{matrix} " \\ \# \\ X_{[0]}^o \\ X_{[1]}^o \end{matrix} \sim \begin{matrix} \mathcal{U}(-5, 5) \\ \mathcal{N}(0, 1) \end{matrix} \tag{19}$$

where $X_{[0]}^o$ and $X_{[1]}^o$ are the random variables from which the observed displacement $x_{[0]}^o$ and velocity $x_{[1]}^o$ states are sampled from. For the reference state’s random variable, we have opted to add a white Gaussian noise with a standard deviation of 1. A terminal time t_f of 2 seconds was considered for the system.

To guide the transient behavior of the system, we have opted for a quadratic Lagrangian function that minimizes that control applied and velocity state over time:

$$L(t, x(t), x_r(t), u(t)) = \frac{1}{2}u(t)^2 + x_{[1]}(t)^2 \tag{20}$$

It should be noted that the system is invariant under all transformations on its sole primitive state $x_{[0]}$ given Definition 2. As such, for the experiments presented, the invariant mask was applied to fix the invariant observed state to zero.

VAN DER POL OSCILLATOR

Van der Pol oscillators were introduced by Balthasar van der Pol to describe the change in current inside a triode that is part of an electronic circuit (Hafeez et al., 2015; Abell and Braselton, 2023). It is second-order, non-conservative, oscillating system with non-linear damping properties. However, Van der Pol oscillators are now used to describes a wide

range of oscillatory processes in a variety disciplines including, but not limited to, modeling irregular heart rate for pace maker design. It is standard benchmark for optimal control by neural controller (Antonelo et al., 2024; Andersson et al., 2012). For our experiments, we have chosen the following variant with the ODE,

$$\mathcal{F}(t, \bar{x}(t), u(t)) = \ddot{x}_{[0]} - 1 - x_{[0]}^2 \quad \dot{x}_{[0]} + x_{[0]} - u = 0 \quad (21)$$

with its corresponding dynamics function f ,

$$\dot{x} = f(x, u) = \begin{matrix} " & \# \\ 1 - x_{[0]}^2 & x_{[1]} \\ x_{[1]} - x_{[0]} + u & \end{matrix} \quad (22)$$

where the primitive state $x_{[0]}$ of the system represents current and u is an external force.

For the observed state distribution used to train the hion controller, we have decided on the following random state vector:

$$\mathbf{X}_o = \begin{matrix} " & \# \\ X_{[0]}^o & \\ X_{[1]}^o & \end{matrix} \sim \begin{matrix} \mathcal{U}(-5, 5) \\ \mathcal{N}(0, 1) \end{matrix} \quad (23)$$

where $X_{[0]}^o$ and $X_{[1]}^o$ are the random variables from which the observed current $x_{[0]}^o$ and change in current w.r.t. time $x_{[1]}^o$ states are sampled from, respectively. For the reference state's random variable, we have also opted to add a white Gaussian noise with a standard deviation of 1. A terminal time t_f of 5 seconds was considered.

For the transient behavior of the Van der Pol oscillator, we considered two distinct set of Lagrangian functions. When trying to reduced the velocity of the system, we used the following quadratic equation:

$$L(t, x(t), x_r(t), u(t)) = \kappa x_{[1]}(t)^2 \quad (24)$$

and, when trying to improve tracking of a reference signal, we used

$$L(t, x(t), x_r(t), u(t)) = \kappa (x_{[0]}(t) - x_r(t))^2 \quad (25)$$

where κ , in both sets, is a scalar hyper-parameter that regulates the intensity of the transient cost.

4.2 Two Point Boundary Value Problem

A Two Point Boundary Value Problem (TPBVP) is an optimal control problem where the system is required to satisfy boundary conditions at both an initial and final time interval. Hion controllers, in their most basic form, can solve these TPBVP where the terminal time t_f is the time by which the final state must be obtained. We can, additionally, not only drive the system towards our desired final state, but also specify the transient behavior we would like the system to have.

Figure 4 illustrates the solution for two different systems obtained by Hion controllers using the T-mano architecture. Fig. 4a shows the solution for a second-order linear system when tasked with minimizing control effort and speed. Fig. 4b presents the solution for

a Van der Pol oscillator when tasked with solely minimizing speed. In both cases, the system was driven to the final state (i.e., the reference state) while maintaining the specified transient profile. For instance, in the case of the Van der Pol oscillator, the system was driven to a constant speed, which was then maintained until the system reached the final state. This represents an optimal solution for minimizing speed.

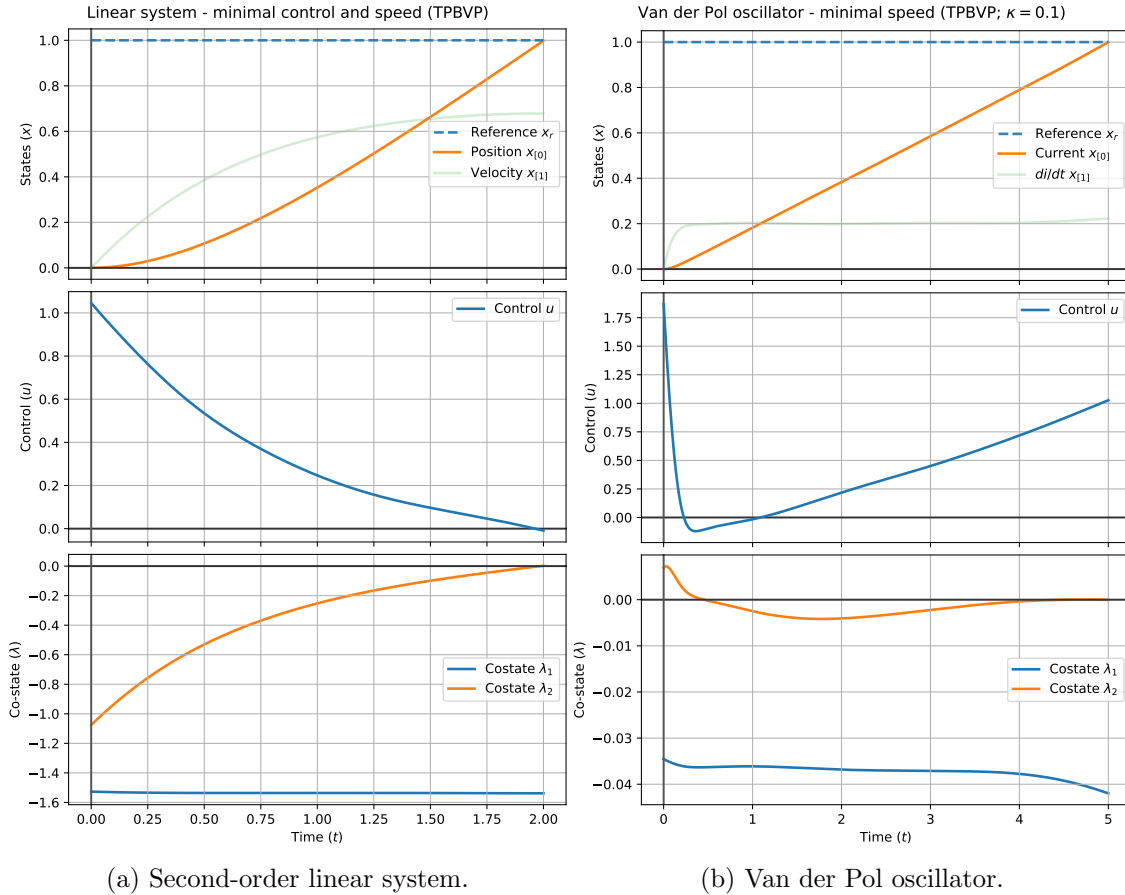


Figure 4: Two point boundary value problem solutions using the T-mano architecture.

4.3 Closed-Loop Control

Hion controllers can be extended to solve control strategies for closed-loop systems. Given the model’s ability to solve TPBVP for variable observed states and reference states, and estimate future states, we can consider closed-loop systems where there is a gap between observation of the state in the environment. This is similar to systems encountered in MPC problems and real-world scenarios where sensors only allow for sparse sampling of the system states. Note that, from now on, each tick on a plot indicates when a new state is observed (i.e., sampled) from the environment.

Figure 5 considers the second-order linear system when controlled to have minimal control and speed as described by the cost function in (20). As seen, T-mano is capable of

driving the system to a reference state while maintaining the optimality requested between sampling periods. Additionally, as the model iteratively obtains the solution to a TPBVP, at the end of each iteration, the reference state is reached unless the reference changes before the next state can be observed. If the reference state x_r is updated before a new state can be observed from the actual environment, then the current estimated state x_h can be assumed to be a new observed state $x_o := x_h$ and the elapsed time \hat{t} is reset to 0. This behavior can be seen when the reference was updated to 0 at $t = 15$ before the next sample of the environment state was captured in the next tick. In this instance, the model moved toward the new reference, and when a new observed state was captured from the actual system, it readjusted its control once again.

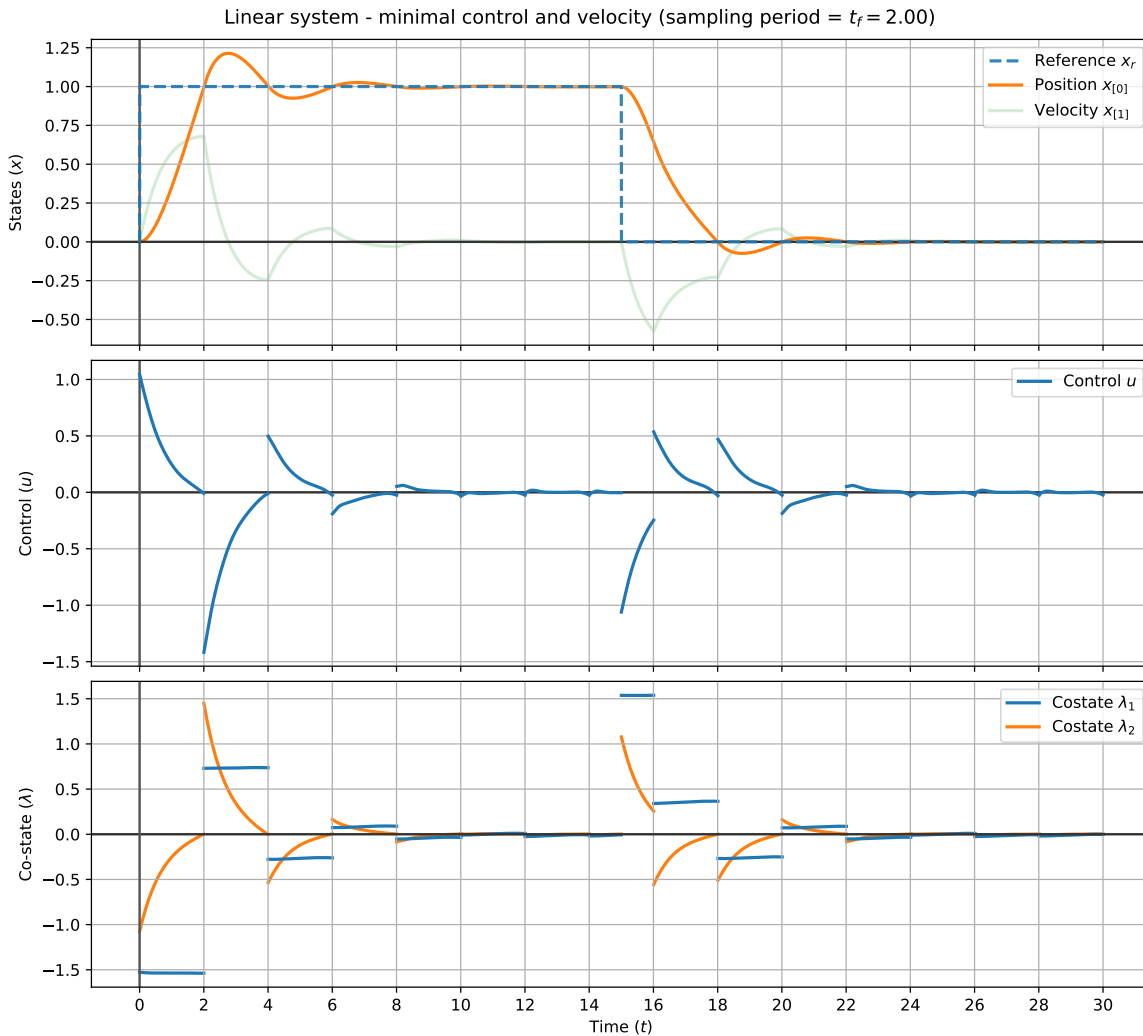


Figure 5: Linear system controlled to minimize the necessary control applied and velocity as a priority.

Fig. 6 presents what occurs when controlling a non-linear Van der Pol oscillator to have minimal speed between observed states. The desired behavior is represented in (24). As

seen, T-mano controls the system to have just the constant speed needed between observed states to reach the reference state before a new state is sampled. This is a known optimal solution to the problem. In the plot, it can also be seen that a maneuver with the controls occurs whenever a new state is sampled. It is speculated that this occurs because, while the reference state may be obtained by the terminal time t_f , some momentum may exist, necessitating a non-linear maneuver to cancel it and stay on the desired course. To a lesser extent, some error between the numerical simulation of the environment and the state estimation emerges, and thus when the numerical simulation is sampled, the model corrects itself to eliminate the error.

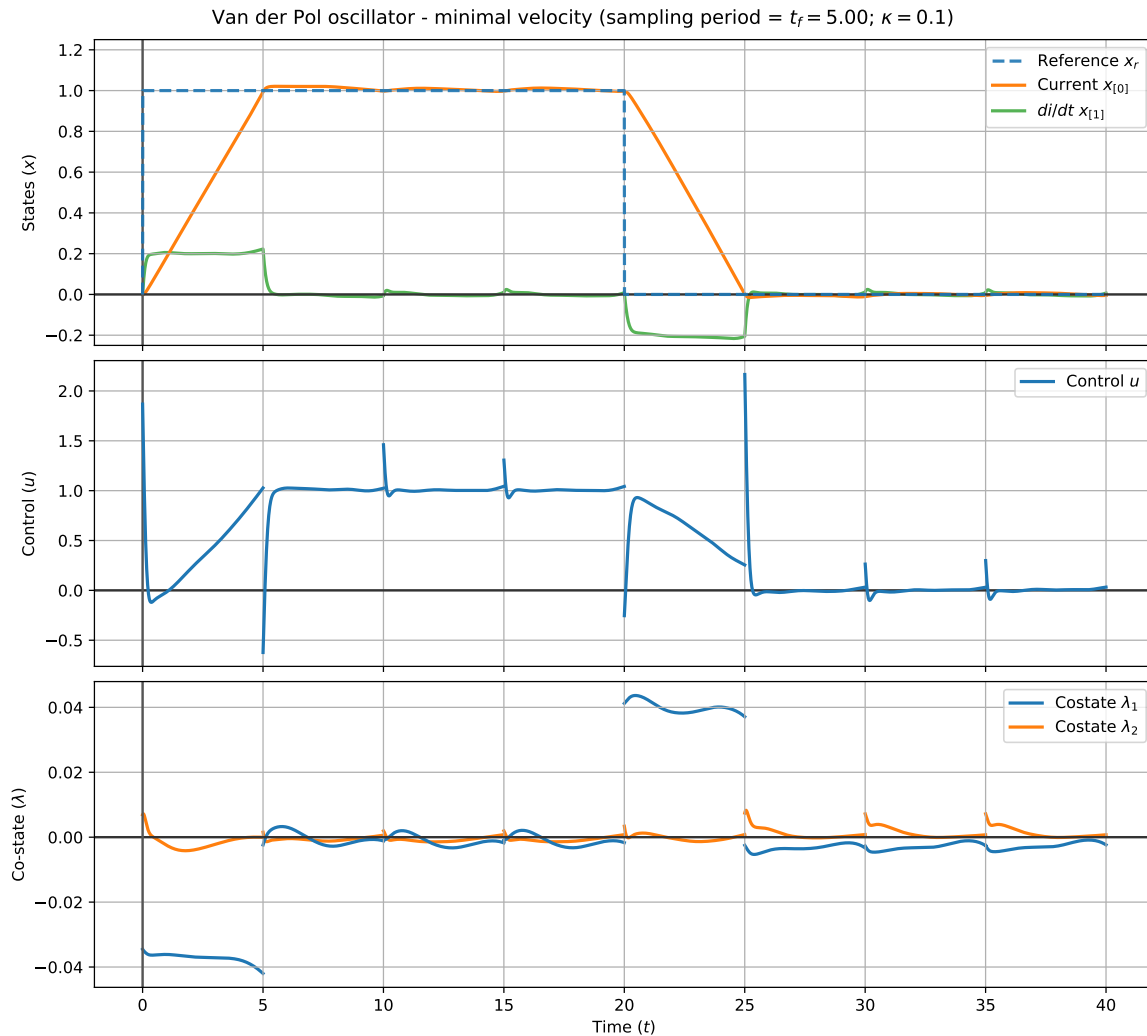


Figure 6: Van der Pol oscillator controlled to have minimal speed between sampling periods as a priority.

In Fig. 7, the tracking problem is explored, where the model is tasked with prioritizing the tracking of the reference state. The objective to prioritize tracking the reference is embedded using the Lagrangian (25). As illustrated, the T-mano model quickly drives

the current state to the reference before the new state is observed and maintains it. This behavior is a departure from that observed in Fig. 6. However, the maneuvering observed when a new state is sampled can still be seen due to the same conditions discussed previously. This time, however, the magnitude of the control is larger, as it is desired that the model bring the system to the reference state rapidly.

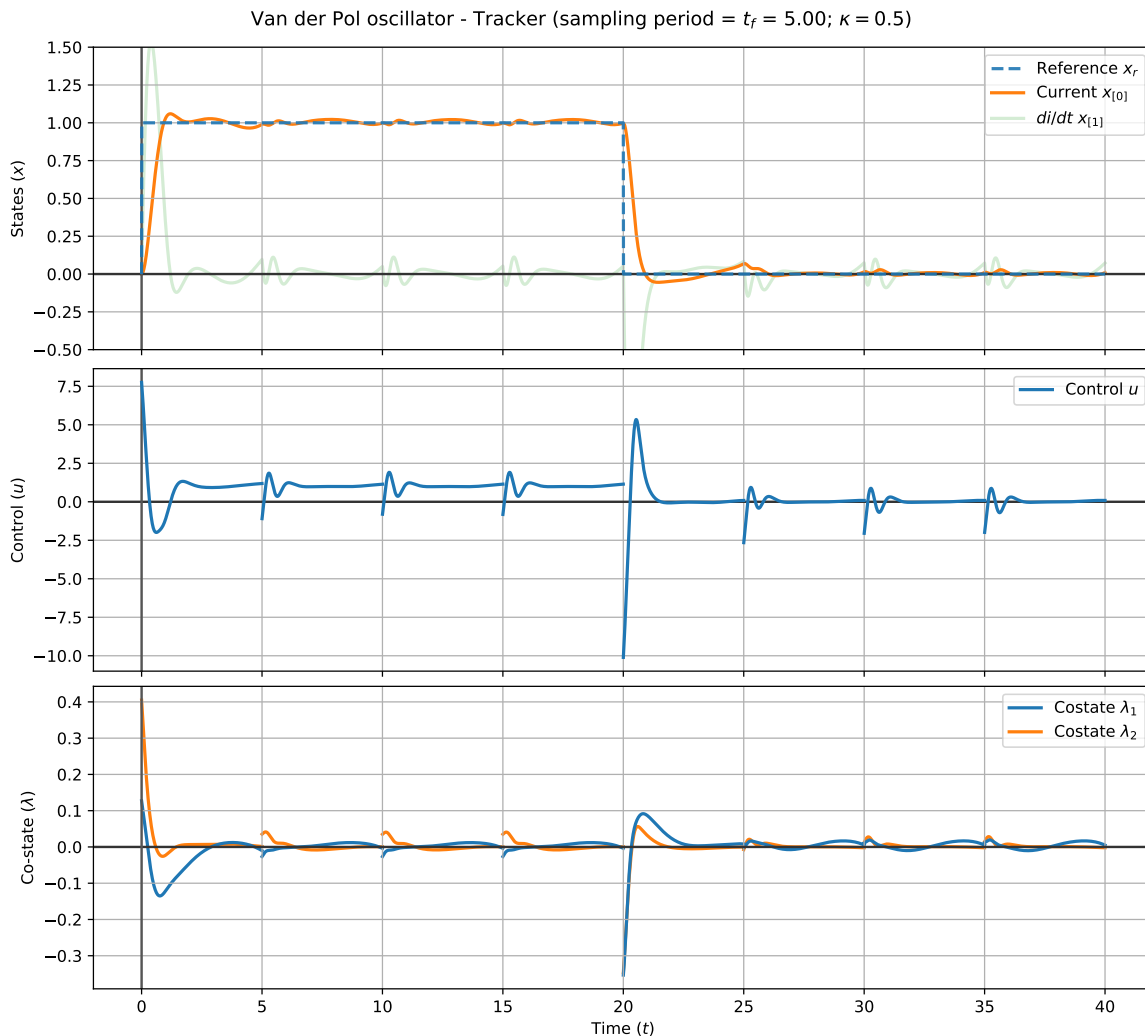


Figure 7: Van der Pol oscillator controlled to follow the reference as a priority.

4.3.1 MODEL-PREDICTIVE CONTROL

Hion controllers can also be used to drive a system towards a reference state using a model-predictive control (MPC) scheme, where the terminal time t_f defines the size of the prediction and control horizon. As sampling periods are shorter than the trained terminal time t_f , the control is based on the concept of steering the system towards a goal at the end of a receding horizon. Note that under sampling may impact the optimality of the controller.

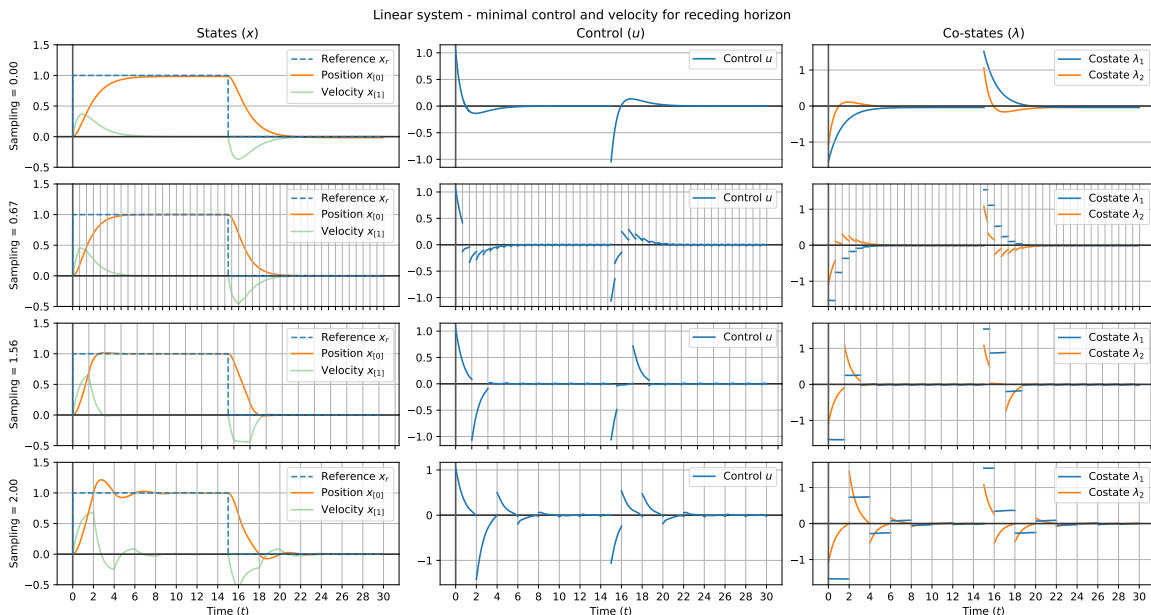


Figure 8: Same linear system controller for different sampling rates.

Additionally, while we showcase states sampled at regular intervals, a mix of sampling rates can be implemented depending on the availability of the environment state.

Fig. 8 presents the behavior of our T-mano model under the MPC scheme for the second-order linear system. As observed, the model is capable of driving the system towards the reference state at distinct sampling rates. When the sampling rate decreases, additional discontinuities in the control and co-states emerge. Interestingly, when the environment is sampled in real-time, the control and co-states exhibit smoothness. It is also observed that the controller takes longer to drive the system to the reference state as the sampling rate decreases.

Fig. 9 showcases the results obtained for the Van der Pol tracker model when considering the MPC scheme. As observed, the controller is capable of driving the system towards the reference state of the non-linear system in most instances when under-sampled. However, unlike the linear system, some maneuvering is observed whenever the environment is sampled due to the non-linear dynamics, the desired transient characteristics, and the micro-adjustments needed due to the small accumulated error between the numerical solver and the model state estimation. Additionally, for a sampling rate of 0.0 (i.e., without any delay in state feedback), it is observed that the model does not control the system towards the reference state. The origin of this behavior is unclear, but it has been linked to the convergence of the losses associated with optimality during training. Finally, the discontinuity and rapid movement that arise in the control when quickly sampled could be challenging to implement in real-world systems and may require smoothness.

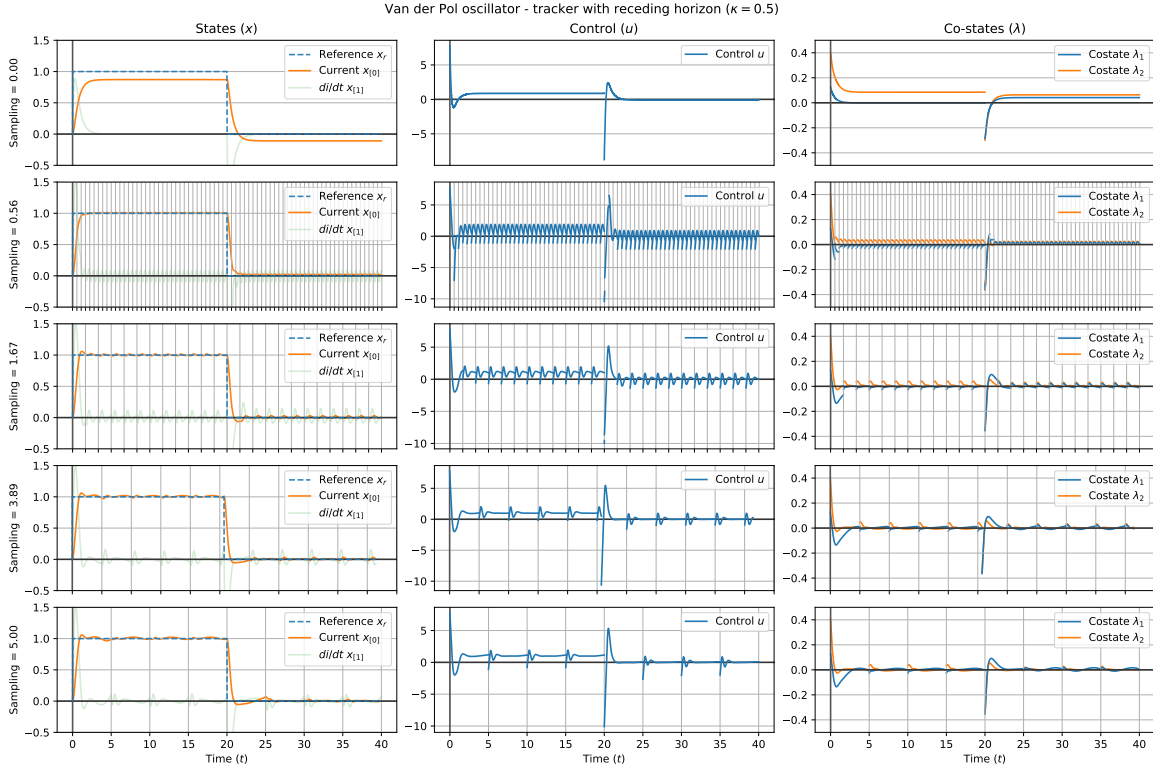


Figure 9: Same Van der Pol oscillator tracker for different sampling rates.

4.4 Fine-Tuning

An attribute of Hion controllers and, in particular, our T-mano models is that once trained, the parameters μ can be easily be fine-tuned through Algorithm 1. It can be fine-tuned for new transient behaviors (given a change to the Lagrangian function), constants in the dynamics, terminal time t_f , and state distributions.

Fig. 10 demonstrate variant T-mano models and their change in behavior when fine-tuned to distinct Lagrangian functions. For these results, the form of the Lagrangian functions tested remained the same but its optimality intensity was modulated by the hyper-parameter k in Eq. (24). As previously discussed, this Lagrangian function seeks to reduce the velocity of the oscillator between sampling periods. When k is decreased, it can be observed weaker optimality for maintaining reduced velocity between sampling, specially once the reference state is reached. It can also be observed that the co-states – which can heuristically be understood as the rate of change towards optimality w.r.t. time – is lower the lesser the intensity for reduced velocity is. Lower values suggest that the model has less interest in maintaining reduced velocity. The results show the T-mano can be fine-tuned for new transilient behavior.

It should also be highlighted that the tracking controllers presented in Fig. 7 and 9 were fined-tuned from the model trained to have minimal velocity between sampling in Fig. 6.

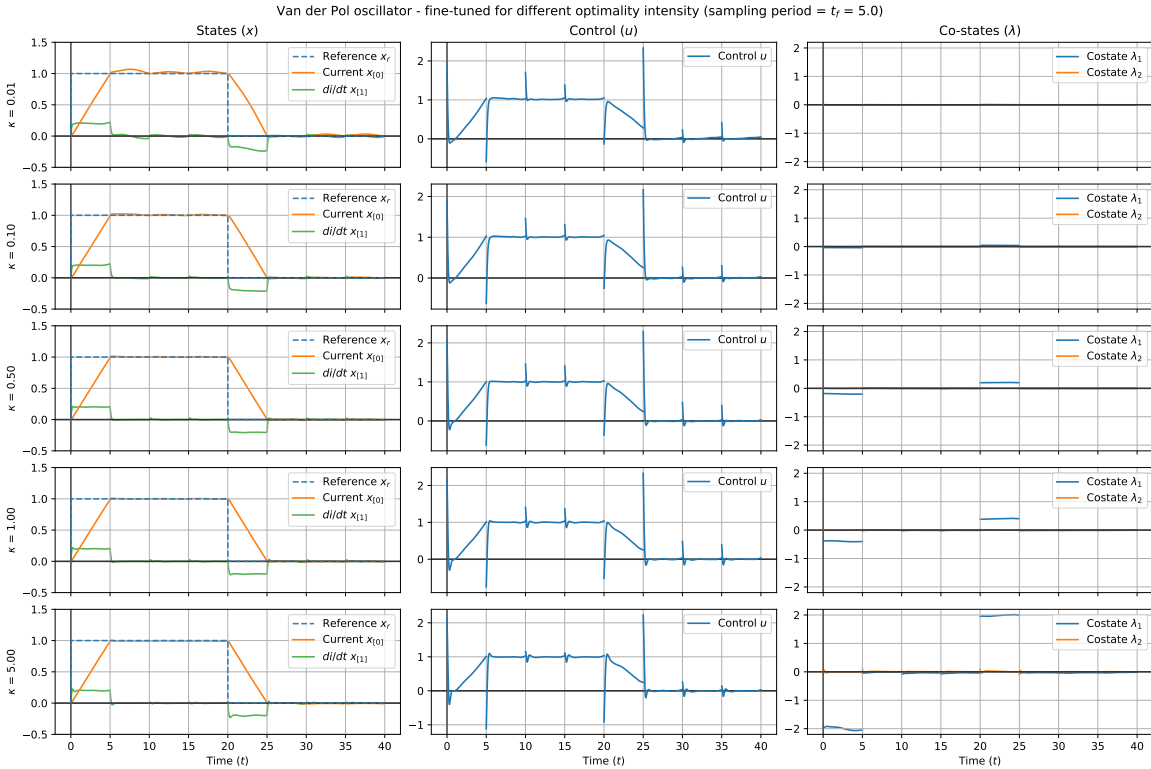


Figure 10: Van der Pol oscillator fine-tuned for different intensity in transient response.

5 Conclusion

This work introduces Hion controllers, a novel class of neural network models designed to achieve two key functionalities: estimating future states of dynamical systems and calculating the optimal control needed to reach desired states. Additionally, we present the T-mano architecture, which ensures accurate initial conditions and system dynamics in the state estimation process, independent of the model parameters values. The source code for this project is publicly available at <https://github.com/wzjoriv/Hion>. Further details regarding the conducted experiments can be provided upon request.

Hion controllers (as modeled by our T-mano architecture) demonstrate significant potential for real-world applications. Firstly, they can be trained to manipulate the transient characteristics of the controlled system. This has significant importance for designing optimal motion trajectories for robots, and finding optimal control inputs for spacecraft maneuvers. For instance, industrial robots in a factory setting can be programmed with our controllers to operate at lower accelerations or speeds while moving around, enhancing safety and mitigating potential collisions. Secondly, Hion controllers excel at estimating future states of an system. This predictive capability empowers proactive collision avoidance and obstacle clearance strategies. It may also facilitate the coordination of multi-agent systems by anticipating the future trajectories of individual agents and their potential interactions points. Additionally, it fosters resilience against state feedback delays and disturbances by leveraging state estimation to remove noise or predict states until a new measurement

becomes available. Lastly, Hion controllers can estimate higher-order time derivatives of states, enabling analysis of properties like jerk, snap, crackle, and pop, and allowing for control over their transient behavior.

However, limitations do exist. Currently, control actions may exhibit discontinuities upon observing new states due to the absence of information regarding higher-order time derivatives in the system. This may be problematic for real-world systems that cannot tolerate sudden changes in control inputs. A potential solution lies in incorporating information about higher-order derivatives of the previous iteration’s state estimation. Another limitation pertains to control scenarios with zero delay between state measurements. In this situation, T-mano models may not drive the system to the reference state contingent to the convergence of the model’s parameters as seen in the results section.

Future research directions are promising. We aim to investigate the application of Hion controllers for control of more complex non-linear chaotic dynamical systems. The ability to predict future states also provides a foundation for collision avoidance strategies in multi-agent systems or complex environments. Additionally, since T-mano models can be made small with few parameters, exploration of their implementation in resource-constrained embedded systems is another compelling avenue. Given higher-order state and control estimation are obtained via differentiability of the model, no additional parameters are also needed to model them. Other future works will explore expanding the T-mano architecture for enhanced state estimation under noisy observed state sampling.

Appendix A. Additional Results

In addition to the ones presented in Section 4, we have included some additional simulations conducted with our proposed T-mano controller for distinct scenarios.

A.1 Stabilization of Second-Order Linear System

Fig. 11 showcases the system dynamics when controlled by the T-mano model to stabilize a second-order linear system that has an initial speed.

A.2 Model-Predictive Control for Minimal Speed of Van der Pol oscillator

Fig. 12 showcases the various dynamics for a Van der Pol oscillator when the environment states are observed at different sampling rates.

References

- M. L. Abell and J. P. Braselton. Chapter 4 - higher-order linear differential equations. In M. L. Abell and J. P. Braselton, editors, *Differential Equations with Mathematica (Fifth Edition)*, pages 115–219. Academic Press, fifth edition edition, 2023. ISBN 978-0-12-824160-8. doi: <https://doi.org/10.1016/B978-0-12-824160-8.00009-7>. URL <https://www.sciencedirect.com/science/article/pii/B9780128241608000097>.
- A. J. Abougarair, H. Almgallesh, and N. A. A. Shashoa. Dynamics and optimal control of quadcopter. In *2024 IEEE 4th International Maghreb Meeting of the Conference on*

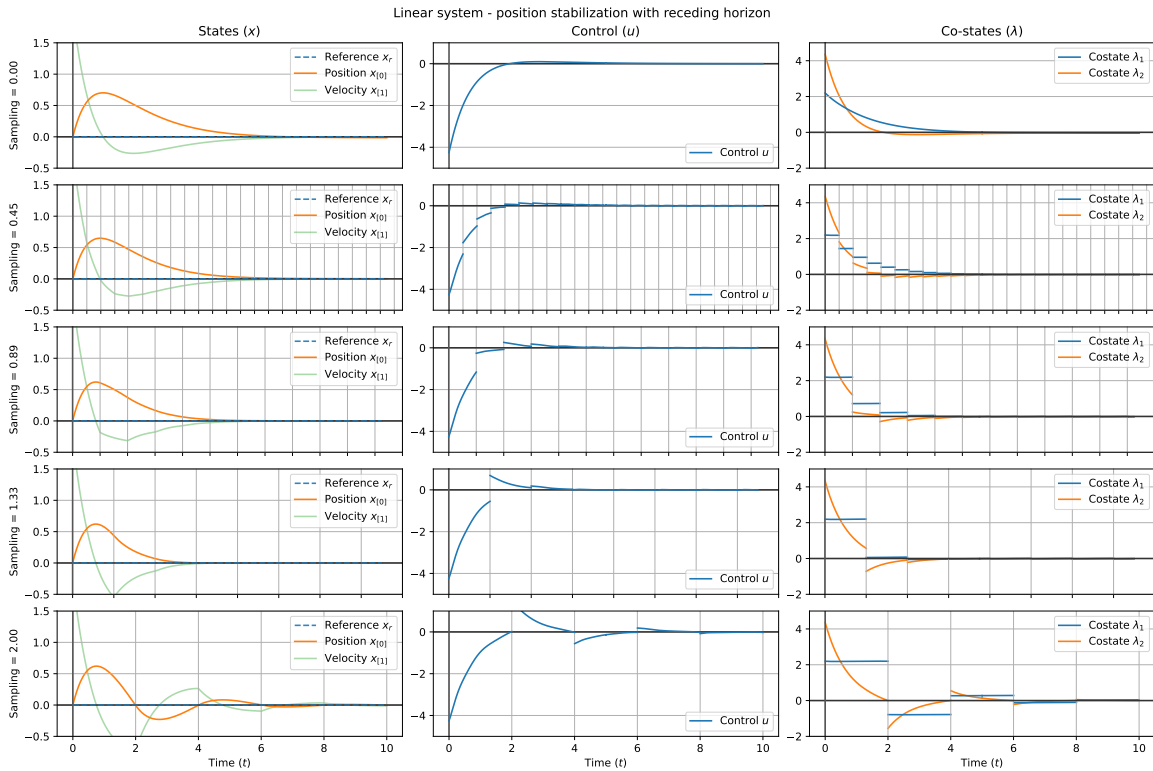


Figure 11: Same linear system controller stabilizing system at different sampling rates.

Sciences and Techniques of Automatic Control and Computer Engineering (MI-STA), pages 136–141. IEEE, 2024.

- B. M. Åkesson and H. T. Toivonen. A neural network model predictive controller. *Journal of Process Control*, 16(9):937–946, 2006.
- J. Andersson, J. Åkesson, and M. Diehl. Dynamic optimization with casadi. In *2012 IEEE 51st IEEE Conference on Decision and Control (CDC)*, pages 681–686. IEEE, 2012.
- E. A. Antonelo, E. Camponogara, L. O. Seman, J. P. Jordanou, E. R. de Souza, and J. F. Hübner. Physics-informed neural nets for control of dynamical systems. *Neurocomputing*, 579:127419, 2024.
- F. Arnold and R. King. State–space modeling for control based on physics-informed neural networks. *Engineering Applications of Artificial Intelligence*, 101:104195, 2021.
- J. Barry-Straume, A. Sarshar, A. A. Popov, and A. Sandu. Physics-informed neural networks for pde-constrained optimization and control. *arXiv preprint arXiv:2205.03377*, 2022.
- A. Bemporad, F. Borrelli, M. Morari, et al. Model predictive control based on linear programming~ the explicit solution. *IEEE transactions on automatic control*, 47(12): 1974–1985, 2002.

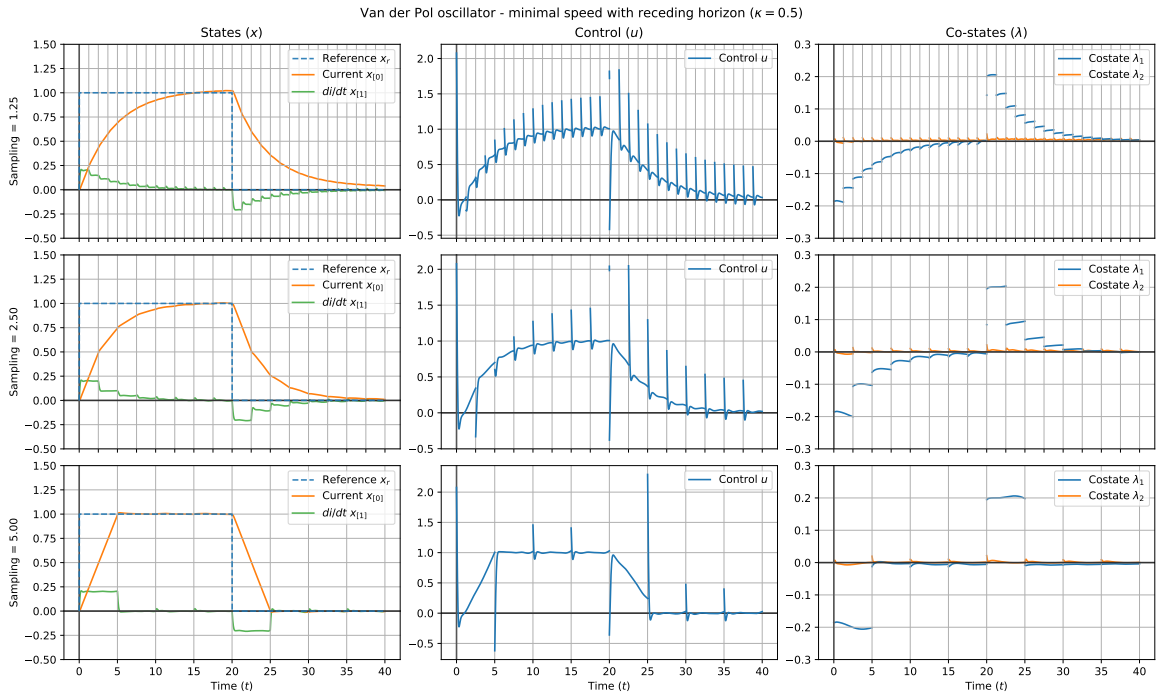


Figure 12: Same Van der Pol system controller for reduced speed at different sampling rates.

L. Cavagnari, L. Magni, and R. Scattolini. Neural network implementation of nonlinear receding-horizon control. *Neural computing & applications*, 8:86–92, 1999.

C. Chi. Nodec: Neural ode for optimal control of unknown dynamical systems. *arXiv preprint arXiv:2401.01836*, 2024.

A. D’ambrosio, E. Schiassi, F. Curti, and R. Furfaro. Pontryagin neural networks with functional interpolation for optimal intercept problems. *Mathematics*, 9(9):996, 2021.

R. R. Faria, B. Capron, A. R. Secchi, and M. B. de Souza Jr. A data-driven tracking control framework using physics-informed neural networks and deep reinforcement learning for dynamical systems. *Engineering Applications of Artificial Intelligence*, 127:107256, 2024.

H. Y. Hafeez, C. E. Ndikilar, and S. Isyaku. Analytical study of the van der pol equation in the autonomous regime. *Progress*, 11:252–262, 2015.

Z. Hao, S. Liu, Y. Zhang, C. Ying, Y. Feng, H. Su, and J. Zhu. Physics-informed machine learning: A survey on problems, methods and applications. *arXiv preprint arXiv:2211.08064*, 2022.

M. Hertneck, J. Köhler, S. Trimpe, and F. Allgöwer. Learning an approximate model predictive controller with guarantees. *IEEE Control Systems Letters*, 2(3):543–548, 2018.

- L. Hewing, K. P. Wabersich, M. Menner, and M. N. Zeilinger. Learning-based model predictive control: Toward safe learning in control. *Annual Review of Control, Robotics, and Autonomous Systems*, 3(1):269–296, 2020.
- I. Hwang. Problem set 3. Class notes, AAE 568 Applied Optimal Control and Estimation, School of Aeronautics and Astronautics, Purdue University, West Lafayette, IN, 2022.
- J. P. Jordanou, E. A. Antonelo, and E. Camponogara. Echo state networks for practical nonlinear model predictive control of unknown dynamic systems. *IEEE transactions on neural networks and learning systems*, 33(6):2615–2629, 2021.
- S. Katayama, M. Murooka, and Y. Tazaki. Model predictive control of legged and humanoid robots: models and algorithms. *Advanced Robotics*, 37(5):298–315, 2023.
- Z. Ma and S. Zou. *Optimal Control Theory*. Springer, 2021.
- A. Naimi, J. Deng, V. Vajpayee, V. Becerra, S. Shimjith, and A. J. Arul. Nonlinear model predictive control using feedback linearization for a pressurized water nuclear power plant. *IEEE Access*, 10:16544–16555, 2022.
- G. F. Oster and E. O. Wilson. *Caste and ecology in the social insects*. Princeton University Press, 1978.
- S. Pang, Y. Zhang, Y. Huangfu, X. Li, B. Tan, P. Li, C. Tian, and S. Quan. A virtual mpc-based artificial neural network controller for pmsm drives in aircraft electric propulsion system. *IEEE Transactions on Industry Applications*, 2023.
- Y. M. Ren, M. S. Alhajeri, J. Luo, S. Chen, F. Abdullah, Z. Wu, and P. D. Christofides. A tutorial review of neural network modeling approaches for model predictive control. *Computers & Chemical Engineering*, 165:107956, 2022.
- J. N. Rivera, J. Ruan, X. Xu, S. Yang, D. Sun, and N. Jain. Fast physics-informed model predictive control approximation for lyapunov stability, 2024. URL <https://arxiv.org/abs/2410.16173>.
- T. Salzmann, E. Kaufmann, J. Arrizabalaga, M. Pavone, D. Scaramuzza, and M. Ryll. Real-time neural mpc: Deep learning model predictive control for quadrotors and agile robotic platforms. *IEEE Robotics and Automation Letters*, 8(4):2397–2404, 2023.
- E. Schiassi, M. De Florio, A. D’Ambrosio, D. Mortari, and R. Furfaro. Physics-informed neural networks and functional interpolation for data-driven parameters discovery of epidemiological compartmental models. *Mathematics*, 9(17):2069, 2021.
- E. Schiassi, A. D’Ambrosio, and R. Furfaro. Bellman neural networks for the class of optimal control problems with integral quadratic cost. *IEEE Transactions on Artificial Intelligence*, 5(3):1016–1025, 2022.
- M. Schwenzer, M. Ay, T. Bergs, and D. Abel. Review on model predictive control: An engineering perspective. *The International Journal of Advanced Manufacturing Technology*, 117(5):1327–1349, 2021.

- E. Todorov. Optimal Control Theory. In *Bayesian Brain: Probabilistic Approaches to Neural Coding*. The MIT Press, 12 2006. ISBN 9780262294188. doi: 10.7551/mitpress/1535.003.0018. URL <https://doi.org/10.7551/mitpress/1535.003.0018>.
- E. Todorov. Lecture notes in pontryagin’s maximum principle, 2012.
- D. Wang, Z. J. Shen, X. Yin, S. Tang, X. Liu, C. Zhang, J. Wang, J. Rodriguez, and M. Norambuena. Model predictive control using artificial neural network for power converters. *IEEE Transactions on Industrial Electronics*, 69(4):3689–3699, 2021.
- B. Winkel. Discover for yourself: An optimal control model in insect colonies. *PRIMUS*, 23(5):459–466, 2013.
- Y. Zheng, C. Hu, X. Wang, and Z. Wu. Physics-informed recurrent neural network modeling for predictive control of nonlinear processes. *Journal of Process Control*, 128:103005, 2023.